Long-range interactions between two 2*s* excited hydrogen atoms

S. Jonsell,[1,2] A. Saenz,[3,*] P. Froelich,[1] R. C. Forrey,[4] R. Côté,[5] and A. Dalgarno[6]
[1]*Department of Quantum Chemistry, Uppsala University, Box 518, S-75120 Uppsala, Sweden*
[2]*NORDITA, Blegdamsvej 17, DK-2100 Copenhagen, Denmark*
[3]*Max-Planck-Institute for Quantum Optics, Hans-Kopfermann-Strasse 1, D-85748 Garching, Germany*
[4]*Berks-Lehigh Valley College, Penn State University, Reading, Pennsylvania 19610-6009*
[5]*Department of Physics, U-3046, University of Connecticut, Storrs, Connecticut 06269*
[6]*Institute for Theoretical Atomic and Molecular Physics, Harvard-Smithsonian Center for Astrophysics, 60 Garden Street, Cambridge, Massachusetts 02138*

(Received 8 November 2001; published 14 March 2002)

The doubly excited $^1\Sigma_g^+$ and $^3\Sigma_u^+$ states of the H_2 molecule converging to the $H(n=2)+H(n'=2)$ limit have been calculated using explicitly correlated basis functions, giving accurate results out to a nuclear separation sufficiently large to apply asymptotic expansions for the potential energy. The autoionization widths have been obtained using the complex-scaling method. For nuclear separations larger than 22 a.u., asymptotic expressions for the interaction energies have been obtained from perturbation theory.

DOI: 10.1103/PhysRevA.65.042501 PACS number(s): 31.10.+z, 34.20.−b

I. INTRODUCTION

After many years of intensive research Bose-Einstein condensation in a gas of spin-polarized hydrogen atoms was finally achieved in 1998 [1]. In this experiment two-photon spectroscopy of the $1s$-$2s$ line was used as a tool to determine the temperature and density of the condensate, through studies of the collisionally shifted and broadened spectral lines [2,3]. The Lyman-α photons from excited metastable hydrogen were detected following a $2s$-$2p$ Stark mixing induced by an electric field. It is important to distinguish this field-induced quenching of the $H(2s)$ state from collisional quenching due to the autoionization reaction $H(2s)+H(2s)\rightarrow H_2^+ + e^-$ and due to excitation transfer $H(2s)+H(2s)\rightarrow H(2p)+H(2p)$, and to understand the effect of these collisions on the linewidth.

There are also prospects for novel sources of excited $H(2s)$ atoms, e.g., through the use of Stark chirped adiabatic passage [4]. This will not only allow direct experimental studies of these excited atoms, but might also deliver a new source of Lyman-α photons, with applications in high-resolution spectroscopy. The rates for collisional quenching determines the maximum density of $H(2s)$ atoms that can be achieved in this type of experiment.

The doubly excited H_2 states describing the collision of two $H(n=2)$ atoms belong to the so-called Q_2 series lying below the $2p\pi_u$ state of H_2^+. Some earlier works have addressed these states [5–7], but to our knowledge this is the first calculation addressing the long-range interactions. Our numerical calculations extend the data previously available from the internuclear distance $R=6$ a.u. to $R=22$ a.u. The calculation includes the width due to autoionization. Asymptotic formulas are given for $R>22$ a.u. Our treatment does not as yet include the fine-structure splitting or Lamb shift. In a recent paper these molecular data have been used to calculate rates for autoionization, excitation transfer, and elastic scattering at thermal temperatures [8].

II. MOLECULAR REGION

The molecular region of interatomic distances is where the atom-atom interaction is too strong to be treated as a small perturbation of the atomic states, and hence has to be determined numerically by means of a molecular calculation. The characteristic radius of a hydrogen atom scales as the square of the principal quantum number n. Hence, for a hydrogen molecule that asymptotically separates into two $n=2$ excited hydrogen atoms the molecular region is about four times larger than for the ground state of H_2. We have found it sufficient to extend the molecular calculations out to $R=22$ a.u. At this nuclear separation the effects of electron exchange are negligible. Two $H(2s)$ atoms can form a molecular state of either $^1\Sigma_g^+$ or $^3\Sigma_u^+$ symmetry. For each of these symmetries there are four states that separate into two $n=2$ excited hydrogen atoms.

A. Electronic autoionization

The states calculated in this work are resonances that can decay through autoionization. For resonances the standard variational principle is not valid. Nevertheless, this principle can be extended to the case of resonances within the complex-scaling approach (see, e.g., the review in [9] and references therein). The complex-scaling operator U is defined through its action on a function f of the coordinate vector $\mathbf{r}$ in three-dimensional space,

$$U(\theta)f(\mathbf{r})=e^{3i\theta/2}f(e^{i\theta}\mathbf{r}). \tag{1}$$

The complex-scaled Hamiltonian $H(\theta)=U(\theta)HU^{-1}(\theta)$ defines an eigenvalue problem

$$H(\theta)c_i^\theta=E_i^\theta c_i^\theta. \tag{2}$$

*Present address: Fachbereich Chemie, Universität Konstanz, Fach M 721, D-78457 Konstanz, Germany.

The complex eigenenergies E_i^θ are of three kinds: (i) bound states, which are unchanged by the complex scaling; (ii) continuum states, which are rotated by an angle 2θ into the complex plane; (iii) resonances, which are uncovered when $\theta > \arg E_i^\theta/2$. The real part of a resonance eigenvalue, $\mathrm{Re}\{E_{\mathrm{res}}\}$, is the energy position of the resonance, and the imaginary part is related to the width Γ of the resonance as $\mathrm{Im}\{E_{\mathrm{res}}\} = -\Gamma/2$.

While in the exact solution of Eq. (2) the resonance eigenvalues will be stationary for $\theta > \arg E_{\mathrm{res}}/2$, any approximate solution using a finite basis will yield an eigenvalue that varies with θ. For resonances the variational principle reduces to a stationarity principle without lower or upper bounds. That is, the optimal scaling angle θ_{opt} is determined *via* the condition that $\theta = \theta_{\mathrm{opt}}$ minimizes the derivative of the energy $dE(\theta)/d\theta$, which in turn determines the complex energy of the resonance $E_{\mathrm{res}} = E(\theta_{\mathrm{opt}})$. For practical purposes in the context of variational calculations it can be shown that the use of the complex-scaled Hamiltonian $H(\theta)$ is equivalent to the use of complex-scaled basis functions. Therefore it is possible to uniquely determine a resonance by requiring maximum stability with respect to a variation of the basis and of the complex-scaling factor θ, but it is impossible to determine a lower or upper bound to the energy position or width of the resonance.

B. Computational details

The application of the complex-scaling approach to molecular systems is not straightforward, since the molecular *Born-Oppenheimer* Hamiltonian is not analytic with respect to dilation. A possible solution to this problem was suggested for diatomic molecules in Ref. [10], where it was demonstrated that by using prolate-spheroidal coordinates $[\xi_i = (r_{iA} + r_{iB})/R, \eta_i = (r_{iA} - r_{iB})/R]$ it is possible to implement *exterior* complex scaling solely by scaling of the electronic coordinates ξ_i.

The calculations were performed using an extended version of a computer program originally written by Kołos and Wolniewicz [11]. The two-electron wave function $\Psi_j(1,2)$ describing state j is expressed in terms of explicitly correlated basis functions as

$$\Psi_j(1,2) = \sum_i c_{i,j}(1 \pm P_{12}) \exp(-\alpha\xi_1 - \overline{\alpha}\xi_2)\xi_1^{r_i}\eta_1^{s_i}\xi_2^{\overline{r}_i}\eta_2^{\overline{s}_i}\rho^{\mu_i} \times [\exp(\beta\eta_1 + \overline{\beta}\eta_2) \pm (-1)^{s_i + \overline{s}_i} \times \exp(-\beta\eta_1 - \overline{\beta}\eta_2)], \quad (3)$$

where the upper sign gives ${}^1\Sigma_g^+$ symmetry and the lower sign gives ${}^3\Sigma_u^+$ symmetry. Here P_{12} is the electron permutation operator, $\rho = 2r_{12}/R$, with r_{12} and R the interelectronic and internuclear distances, respectively, $r_i, s_i, \overline{r}_i, \overline{s}_i, \mu_i$ are integers, and $\alpha, \beta, \overline{\alpha}, \overline{\beta}$ are real numbers. The coefficients $c_{i,j}$ are determined through the diagonalization of the generalized eigenvalue problem.

As discussed in Sec. II A the variational principle cannot be applied for resonances, but instead we use the complex-scaling method. One possible and practical approach to determining resonances within the complex-scaling framework is to perform as a first step a number of real-scaling calculations in order to be able to select a range of real-scaling factors ϱ, where optimal stability of the position of the resonance is observed. After fixing the real-scaling parameter to a value ϱ_{opt} in this regime, a variation of the phase θ of the scaling factor is performed as a second step of the calculation.

In the present calculation the stability of the real energies of the resonances was investigated through the scaling of ξ_1 and ξ_2, which for practical reasons was performed by the equivalent procedure of an inverse scaling of the exponents α and $\overline{\alpha}$ in Eq. (3) by a real parameter. Values of the nonlinear parameters giving a good stability under this scaling were sought for integer values of R, using as a starting point the 249-term basis from Ref. [12]. It turns out that it is very difficult, especially at short internuclear distances, to make a very precise determination of the best possible nonlinear parameters. Instead, approximate values of $\alpha, \beta, \overline{\alpha}, \overline{\beta}$ where all four resonances showed good stability were determined. Sometimes several sets were used for a single value of R, in order to be able to assess the accuracy of the results. The nonlinear parameters at noninteger values of R were obtained by an interpolation of the optimal exponents determined at integer values of R.

In the next step new refined basis sets were obtained by testing a large number of sets of integer exponents $\{\mu_i; r_i, s_i, \overline{r}_i, \overline{s}_i\}$, and discarding those terms that had only a small effect on the energies of the resonances. Using the sets of integer exponents obtained, together with the nonlinear parameters optimized before, we arrived at our final basis sets. In this way we created for each symmetry three different basis sets covering different R intervals, limited in size by the linear dependence caused by the finite numerical precision of the calculation. In the case of ${}^1\Sigma_g^+$ symmetry the basis-set sizes were 380, 430, and 250 for $R < 6$, $6 \leqslant R \leqslant 12$, and $R > 12$ a.u., respectively, and in the case of ${}^3\Sigma_u^+$ symmetry 330, 380, and 300 for $R < 7$, $7 \leqslant R < 13$, and $R \geqslant 13$ a.u. In the outermost region we used different basis sets with separately optimized sets of integer exponents for each state, while in the inner regions the same set of integer exponents was used for all four states of the same symmetry. At the boundaries of the range of R we considered, we did, however, have to reduce successively the size of our basis sets in order to avoid linear dependence in the basis.

The complex resonance energies were obtained using the complex-scaling operation $\xi_i, \eta_i \rightarrow \varrho e^{i\theta}\xi_i, \eta_i$ in the way introduced and described in Ref. [13]. For this purpose the basis-set parameters α and $\overline{\alpha}$ are modified in such a way that they contain the previously determined ϱ_{opt}, i.e., a calculation with $\varrho = 1.0$ (and $\theta = 0.0$) yields now optimal stability of the resonant energy on the real axis. Then the Hamiltonian matrix is calculated for a number of *real* values of the scaling parameter ϱ. Each matrix element is then fitted to a polynomial in ϱ, which can be analytically continued into the complex plane, and thus gives the matrix element at *complex* values of $\gamma = \varrho \exp(i\theta)$. The generalized eigenvalue problem

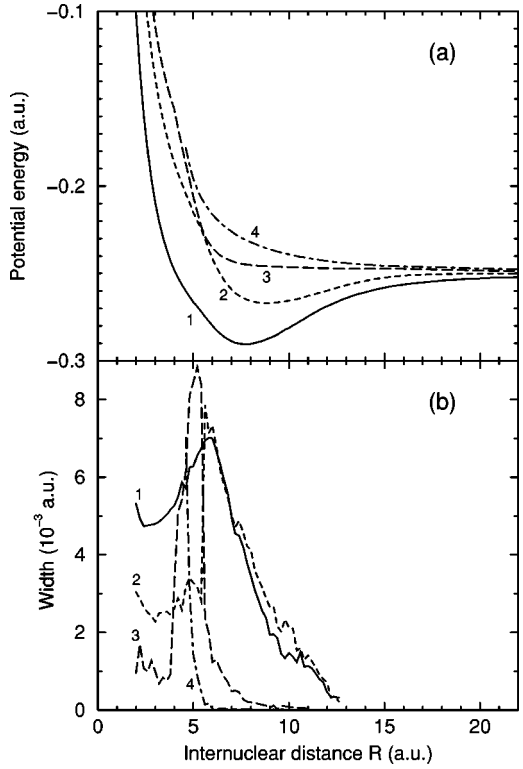

FIG. 1. Potential energies (a) and widths (b) for the $^1\Sigma_g^+$ states that correlate to $n=n'=2$ atomic states.

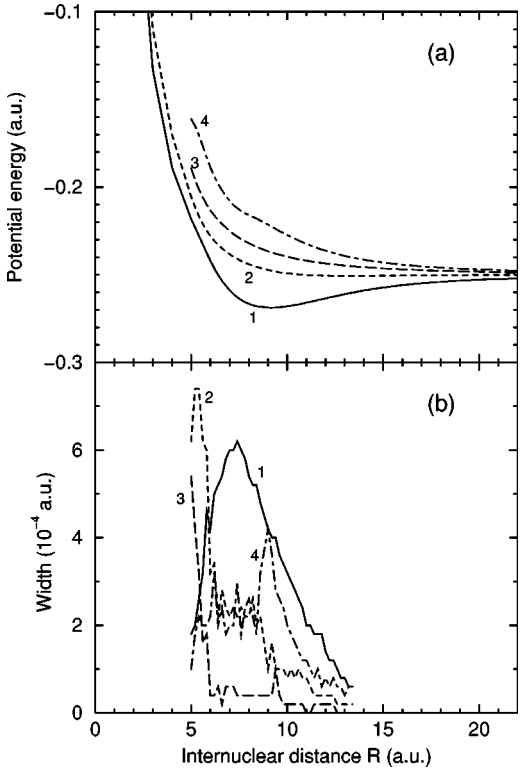

FIG. 2. Potential energies (a) and widths (b) for the $^3\Sigma_u^+$ states that correlate to $n=n'=2$ atomic states.

of this *complex symmetric* Hamiltonian is then solved for a series of θ values. The complex energy of the resonance is determined from the minimum value of $dE/d\theta$. After numerous tests we found that the best results were obtained by using a real grid of 15 ϱ values in the interval 0.86–1.14 in steps of 0.02 on the real axis and by fitting each matrix element to a fourth-order polynomial.

C. Results

The electronic potentials and autoionizing widths obtained are presented in Fig. 1 for $^1\Sigma_g^+$ symmetry and Fig. 2 for $^3\Sigma_u^+$ symmetry. Only states having the asymptotic energy -0.25 a.u. are displayed. We find two binding and two nonbinding states of each symmetry.

An avoided crossing between the second and third $^1\Sigma_g^+$ states at $R\simeq 5.5$ a.u. is clearly visible in Fig. 1. Also the corresponding autoionization widths show a striking change of character at this internuclear distance. Further avoided crossings occur at shorter internuclear distances. In particular, a fifth more highly excited state correlating to the $n=3,n'=2$ threshold, and consequently not displayed in Fig. 1, crosses the fourth state at $R\simeq 4.5$ a.u. Our basis sets, being optimized for states correlating to the $n=n'=2$ threshold, did not give a good description of this more highly excited state. Therefore we have not continued our calculation of state 4 inside this avoided crossing. For the $^3\Sigma_u^+$ symmetry a similar avoided crossing between the fourth state and a more highly excited state occurs already at $R\simeq 8.6$ a.u.

The molecular states discussed in this paper were recently calculated in the range $0\leqslant R\leqslant 6$ a.u. by Sanchez and Martin [7] using the method of Feshbach projectors. In this method the H_2 states are expanded in a basis of bound and continuum one-electron orbitals of H_2^+. The H_2^+ orbitals were calculated in a one-center basis built on B splines. This method is known to be accurate at short internuclear distances and has advantages in facilitating a physical interpretation of the molecular states. This method can, however, not be used for large internuclear distances because the one-center approach used runs into numerical problems for increasing internuclear distances.

Our method, on the other hand, being based on prolate-spheroidal coordinates that by definition are centered on both nuclei, gives accurate results out to an internuclear distance sufficiently large to apply the asymptotic forms described in Sec. III. In principle, our method is also well suited for calculations at short internuclear distances, since it very efficiently incorporates electronic correlation. The ground state of H_2 has been accurately calculated at $R=0.2$ a.u. using a 249-term basis of the same type as ours [12]. When considering the doubly excited states, however, the situation is quite complicated at short internuclear distances, since there are many closely lying states and many avoided crossings. In fact, at short distances the states we have calculated have energies less than the $2p\sigma_u$ state of H_2^+, under which there is a Rydberg series containing an infinite number of states that will be crossed. Hence, to accurately determine the doubly excited states at short internuclear distances it is not sufficient to use, as we have done, the same basis set for all states of the same symmetry. Instead, for each state one would have to carefully optimize an individual basis set. Ad-

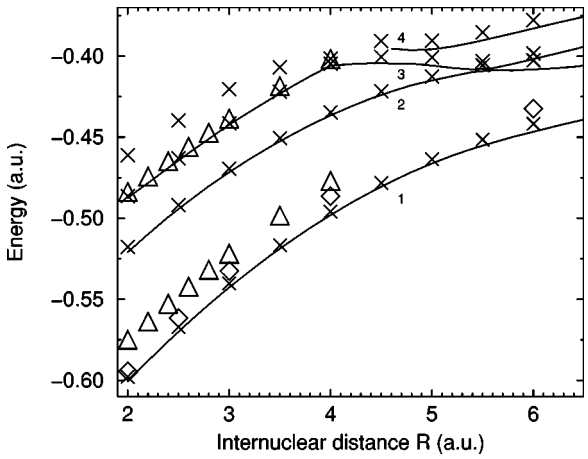

FIG. 3. Comparison of our results for potentials of the $^1\Sigma_g^+$ states (solid lines) to the results in Ref. [7] (crosses), Ref. [6] (triangles), and Ref. [5] (diamonds).

ditionally, since the states rapidly change character when R is decreased and avoided crossings are encountered, this optimization would have to be repeated at each internuclear distance. Since our main interest has been the long-range interactions we have not found it worthwhile to go through this very elaborate procedure.

In the region of R where our calculations overlap with those of Sanchez and Martin, comparisons of the results have been made in Figs. 3 and 4. The comparisons also include results by Guberman [5] and Tennyson [6]. Our results for the $^1\Sigma_g^+$ states agree very well with the results of Sanchez and Martin. We confirm their conclusion that the energy of state 1 calculated by Tennyson is somewhat too high. Also our width of state 1 agrees closely with Sanchez and Martin, while Tennyson obtained a larger width. For $^3\Sigma_u^+$ symmetry our calculation only extends down to $R=5$ a.u., limiting the opportunities for comparisons with earlier works. We note that our energies are significantly lower than those of Sanchez and Martin for all four states. Usually this is taken as a sign of better accuracy, but as noted in Sec. II B this need not necessarily be true for calculations of resonances. For the widths we note that our results for the second state of $^3\Sigma_{u^+}$ symmetry are significantly smaller than the results of Sanchez and Martin. All in all, considering that very different computational approaches have been used, we find that the agreement with the data of Sanchez and Martin is remarkably good. This gives us confidence in our results for $R>6$ a.u., especially, since better stability of the eigenvalues was observed for larger internuclear distances.

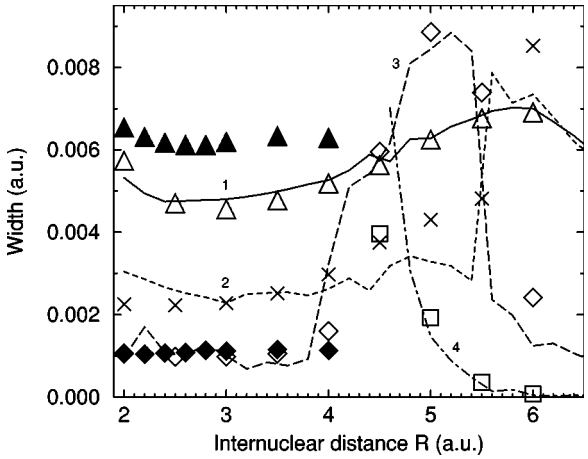

FIG. 4. Same as Fig. 3 but for the widths. Lines show our data coded as in Fig. 1. Results from [7]: state 1 (open triangles), state 2 (crosses), state 3 (open diamonds), state 4 (squares). Results from [6]: state 1 (filled triangles), state 3 (filled diamonds).

III. ASYMPTOTIC REGION

In this section we shall discuss the asymptotic molecular states in terms of atomic states with well-defined orbital angular momentum l,m_l and spin s,m_s. This means that the spin-orbit interaction will be ignored here, an approximation that is valid when the collision energy is higher than the fine-structure splitting of the hydrogen atom, 4.5×10^{-5} eV$=0.53$ K. Hence the $2s$ and $2p$ states of the hydrogen atom are approximated as being degenerate in energy. At large internuclear distances the wave function will approach a product of two atomic states (or rather, as will be seen below, a linear combination of such products). For sufficiently large internuclear distances the molecular potential energies may then be calculated analytically treating the electrostatic atom-atom interaction by perturbation theory. The resulting asymptotic potential-energy curve has the form

$$E(R)=\frac{C_3}{R^3}+\frac{C_5}{R^5}+\frac{C_6}{R^6}+\frac{C_8}{R^8}+\cdots, \tag{4}$$

where the C_3 and C_5 terms come from first-order perturbation theory, and are nonvanishing as a result of the degeneracy of the $2s$ and $2p$ states, while the C_6 and C_8 arise from second-order perturbation theory, and are present even if the degeneracy is lifted.

A. Exchange

The atom-atom interaction contains also a contribution from the exchange of the two electrons. At large internuclear distances this contribution vanishes exponentially, i.e., faster than the electrostatic interaction. The exchange contribution is difficult to treat consistently in perturbation theory. In the following section we shall show how this contribution may be extracted from our numerical data.

We denote the product state of two noninteracting $n=2$ hydrogen atoms A and B by $|2l_I2l'_{I'}\rangle$. Here l,l' specify the angular momentum, the subscripts $I,I'=A,B$ denote to which hydrogen atom the orbital belongs, and the ordering reflects which electron is occupying the orbital, i.e., "electron 1" belongs to the first orbital and "electron 2" to the second.

The molecular Hamiltonian is invariant under inversion i of all electronic coordinates, electron exchange P_{12}, and reflection in a plane containing the nuclei. Let $p=\pm1$ be the parity under inversion (*gerade* or *ungerade* symmetry), and

$\sigma=\pm 1$ the parity under exchange (singlet or triplet symmetry). From an atomic product state $|2l_A 2l'_B\rangle$ one may then generate asymptotic orbitals adapted to the molecular symmetries (symmetrization with respect to reflection is not included):

$$|\Psi_{\rm mol}\rangle=\frac{1}{2\sqrt{1+\delta_{ll'}}}[|2l_A 2l'_B\rangle+p\sigma(-1)^{l+l'}|2l'_A 2l_B\rangle + \sigma|2l'_B 2l_A\rangle+p(-1)^{l+l'}|2l_B 2l'_A\rangle]. \quad (5)$$

In this work we are primarily interested in the interaction between two $2s$ atoms. Hence, the relevant orbitals are those with ${}^1\Sigma_g^+$ and ${}^3\Sigma_u^+$ symmetries (in the case of spin-polarized hydrogen only the latter symmetry is relevant since all collisions will then have triplet spin). There are four orbitals of each symmetry converging to the $n=n'=2$ threshold. These are degenerate asymptotically (if spin-orbit interaction is ignored), but not for finite R. The actual molecular states correlate not to single products of atomic states, but to linear combinations. Hence, we cannot focus only on the $|2s_A,2s_B\rangle$ asymptote. The molecular interaction couples the $2s$ and $2p$ atomic states, and hence there is a possibility for $2s\rightarrow 2p$ transitions to occur in elastic $2s$-$2s$ collisions. The structure of Eq. (5) will still remain valid for the actual asymptotic molecular states, although each term $|2l_A 2l'_B\rangle$ will be replaced by a linear combination of such terms.

Using a symmetry-adapted molecular orbital of the form in Eq. (5), the expectation value of the Hamiltonian is

$$\langle\Psi_{\rm mol}|H_{\rm mol}|\Psi_{\rm mol}\rangle=\frac{1}{1+\delta_{ll'}}[\langle 2l_A 2l'_B|H_{\rm mol}|2l_A 2l'_B\rangle + p\sigma(-1)^{l+l'}\langle 2l_A 2l'_B|H_{\rm mol}|2l'_A 2l_B\rangle + \sigma\langle 2l_A 2l'_B|H_{\rm mol}|2l'_B 2l_A\rangle + p(-1)^{l+l'}\langle 2l_A 2l'_B|H_{\rm mol}|2l_B 2l'_A\rangle]. \quad (6)$$

The first two terms are the direct contributions to the energy, which will be treated by perturbation theory in the following section, and the last two terms are the exchange contributions. Although approximate analytical formulas valid for large R exist for the exchange terms [14] these are quite involved, and here we shall instead extract the exchange contribution from our numerical data.

The way to extract the exchange contribution is easy to infer from the form of Eq. (6). For ${}^1\Sigma_g^+$ symmetry one has $p=\sigma=1$, while for ${}^3\Sigma_u^+$, $p=\sigma=-1$. Hence, we see from Eq. (6) that for a ${}^1\Sigma_g^+$, ${}^3\Sigma_u^+$ pair of states that asymptotically separate to the same combination of atomic orbitals, the direct contributions are identical, while the exchange contributions differ by a factor -1. Hence, the difference in energy of the two states equals twice the exchange contribution. The exchange contributions for the four pairs of states calculated in Sec. II are displayed in Fig. 5.

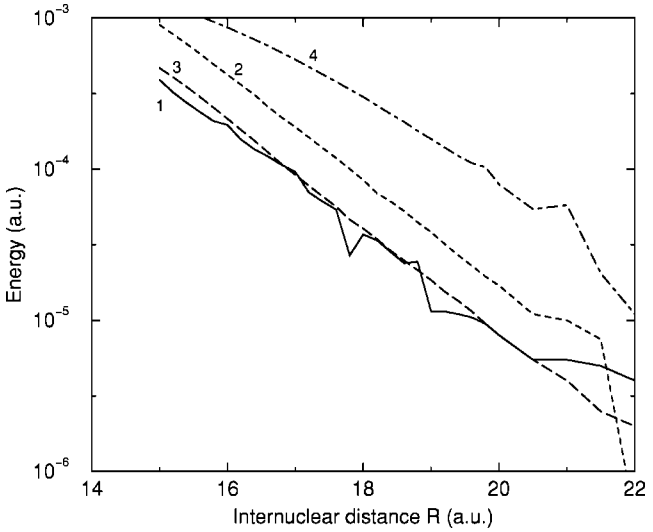

FIG. 5. Exchange contribution of state 1 (solid), state 2 (dashed), state 3 (long dashed), and state 4 (dash-dotted).

We see that the exchange contributions are smooth, exponentially decreasing curves. Some jitter on the level of 10^{-5} a.u. due to numerical inaccuracies can be observed at very large R. However, the exchange contributions clearly show the expected exponential decrease with distance. Considering that the exchange contribution is a very small energy difference that has been extracted from two nearly degenerate states, these results indicate good accuracy for our calculations all the way out to $R=22$ a.u.

At $R=22$ a.u. the exchange energies are of the order of 10^{-5} a.u. or less, while the total binding energies are of the order of 10^{-3} a.u. (the only exception being the second state that has a binding energy 7.6×10^{-5} a.u. and an exchange energy 10^{-6} a.u.). Hence, for $R\geqslant 22$ a.u. the exchange effects give a negligible contribution to the total energy. In the following sections we shall, therefore, ignore exchange when we develop asymptotic formulas for the potential energies.

B. Long-range interaction

In this section we shall look at the contributions to the potential energy arising from first-order perturbation theory in the electrostatic atom-atom interaction. Since the molecule dissociates into neutral atoms the interaction will be of dipole, and higher multipole, type. For the molecular ground state, dissociating into two ground-state atoms possessing no dipole moment, the energy correction from first-order perturbation theory vanishes. The same is true for hydrogen atoms in the $2s$ state. We shall, however, see that through the degeneracy with the $2p$ state, a first-order energy shift appears. In fact, due to the previously mentioned mixing induced by the interaction, the asymptotic molecular states turn out to be *linear combinations* of the different symmetry-adapted molecular orbitals.

At large internuclear distances the interaction of the two atoms may be treated as a perturbation, $H_{\rm mol}=H_{\rm atoms}+V$, where V can be expressed in a multipole expansion

$$V=\frac{1}{R}-\frac{1}{r_{1B}}+\frac{1}{r_{12}}-\frac{1}{r_{2A}}$$
$$=\sum_{l=2}^{\infty}\frac{4\pi}{R^{l+1}}\sum_{l_1,l_2=1}^{l_1+l_2=l} r_1^{l_1}(-r_2)^{l_2}$$
$$\times\sqrt{\frac{2l!}{(2l_1+1)!(2l_2+1)!}}$$
$$\times\sum_{m=-\min\{l_1,l_2\}}^{\min\{l_1,l_2\}}\langle l0|l_1 m l_2 -m\rangle Y_{l_1 m}(\hat{\mathbf{r}}_1)Y_{l_2 -m}(\hat{\mathbf{r}}_2), \tag{7}$$

where Y_{lm} is the spherical harmonic and $\langle lm|l_1m_1l_2m_2\rangle$ are Clebsch-Gordan coefficients. The leading term in the expansion (7) is $l=2$, giving a contribution proportional to $1/R^3$,

$$V_3=\frac{1}{R^3}(\mathbf{r}_1\cdot\mathbf{r}_2-3z_1z_2). \tag{8}$$

The next contribution comes from $l=4$, giving a contribution proportional to $1/R^5$. In the basis of the four degenerate $^1\Sigma_g^+$ or $^3\Sigma_u^+$ molecular orbitals $|2s2s\rangle$, $|2p^02p^0\rangle$, $(1/\sqrt{2})(|2s2p^0\rangle-|2p^02s\rangle)$, and $(1/\sqrt{2})(|2p^+2p^-\rangle+|2p^-2p^+\rangle)$ the first-order perturbation matrix (without exchange) up to $l=4$ is

$$\tilde{V}=\begin{pmatrix} 0 & -18/R^3 & 0 & -9\sqrt{2}/R^3 \\ -18/R^3 & 864/R^5 & 0 & 432\sqrt{2}/R^5 \\ 0 & 0 & 18/R^3 & 0 \\ -9\sqrt{2}/R^3 & 432\sqrt{2}/R^5 & 0 & 432/R^5 \end{pmatrix}. \tag{9}$$

Diagonalization of $\tilde{V}$ gives the four asymptotic eigenenergies

$$E_1=-\frac{9\sqrt{6}(\sqrt{864+R^4}-12\sqrt{6})}{R^5}\simeq-\frac{9\sqrt{6}}{R^3}+\frac{648}{R^5},$$

$$E_2=0,$$

$$E_3=\frac{18}{R^3},$$

$$E_4=\frac{9\sqrt{6}(\sqrt{864+R^4}+12\sqrt{6})}{R^5}\simeq\frac{9\sqrt{6}}{R^3}+\frac{648}{R^5}, \tag{10}$$

and the corresponding asymptotic eigenfunctions are, to leading order [that is, if terms proportional to $1/R^5$ in Eq. (9) are neglected],

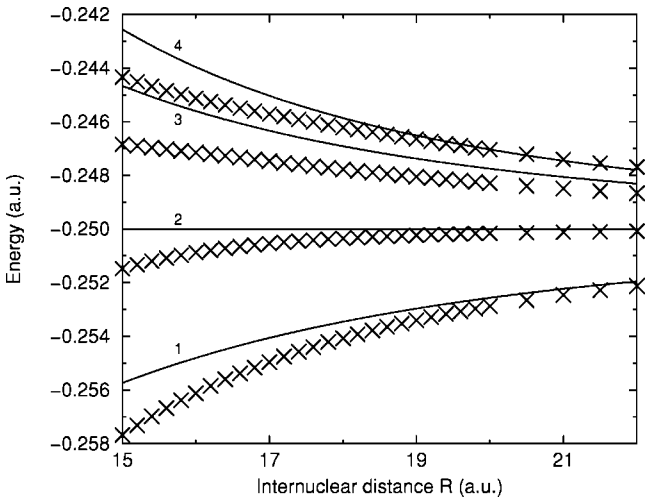

FIG. 6. Numerical energies after removing the exchange contribution (crosses) compared to asymptotic energies from first-order perturbation theory (lines).

$$|1\rangle=\frac{1}{\sqrt{2}}|2s2s\rangle+\frac{1}{\sqrt{3}}|2p^02p^0\rangle+\frac{1}{\sqrt{12}}(|2p^+2p^-\rangle+|2p^-2p^+\rangle), \tag{11}$$

$$|2\rangle=\frac{1}{\sqrt{3}}(|2p^02p^0\rangle-|2p^+2p^-\rangle-|2p^-2p^+\rangle),$$

$$|3\rangle=\frac{1}{\sqrt{2}}(|2s2p^0\rangle-|2p^02s\rangle),$$

$$|4\rangle=\frac{1}{\sqrt{2}}|2s2s\rangle-\frac{1}{\sqrt{3}}|2p^02p^0\rangle-\frac{1}{\sqrt{12}}(|2p^+2p^-\rangle+|2p^-2p^+\rangle).$$

In Fig. 6 the asymptotic expressions for the energies are compared to the numerical data after removing the exchange energy as explained in Sec. III A. We find that the asymptotic energies accurately join the numerical results at $R=22$. Hence, our calculation in combination with the results in [7] gives the molecular energies all the way from $R=0$ out to nuclear separations where fine structure and Lamb shift become important.

IV. CONCLUSIONS

We have calculated the energies and widths of the four $^1\Sigma_g^+$ and the four $^3\Sigma_u^+$ states asymptotically converging to the energy -0.25 a.u., characteristic of the $n=2,n'=2$ atomic states. For short ($R<6$ a.u.) internuclear distances, our results agree well with those of Sanchez and Martin [7].

We are not aware of any previous calculation of these states for larger internuclear distances. We have calculated analytically the asymptotic energies of these states in first-order perturbation theory. From our numerical data we extracted the exchange energy and we conclude that it is less than 10^{-5} a.u. for $R>22$ a.u.

In a future work we will include the effects of spin-orbit coupling and the Lamb shift in our asymptotic formulas. This will allow us to extend our calculations of the collisional quenching of the H(2*s*) state at finite temperatures (larger than a few kelvin) [8] into the regime of ultracold collisions, relevant for Bose-Einstein condensation in hydrogen.

ACKNOWLEDGMENTS

The research of R.C.F. and P.F. was supported by the Natural Science Foundation through a grant for the Institute for Theoretical Atomic and Molecular Physics at Harvard University and at the Smithsonian Astrophysical Observatory. P.F. acknowledges support from the Swedish Natural Science Research Council. The research of R.C.F. was supported by NSF Grant No. PHY-0070920, that of R.C. by NSF Grant No. PHY-9970757, and that of A.D. by the Chemical Sciences, Geosciences and Biosciences Division of the Office of Basic Energy Science, U.S. Department of Energy.

[1] D.G. Fried, T.C. Killian, L. Willmann, D. Landhuis, S.C. Moss, D. Kleppner, and T.J. Greytak, Phys. Rev. Lett. **81**, 3811 (1998).
[2] C.L. Cesar, D.G. Fried, T.C. Killian, A.D. Polcyn, J.C. Sandberg, I.A. Yu, T.J. Greytk, D. Kleppner, and J.M. Doyle, Phys. Rev. Lett. **77**, 255 (1996).
[3] T.C. Killian, D.G. Fried, L. Willmann, D. Landhuis, S.C. Moss, T.J. Greytak, and D. Kleppner, Phys. Rev. Lett. **81**, 3807 (1998).
[4] L.P. Yatsenko, B.W. Shore, T. Halfmann, K. Bergmann, and A. Vardi, Phys. Rev. A **60**, R4237 (1999).
[5] S.L. Guberman, J. Chem. Phys. **78**, 1404 (1983).
[6] J. Tennyson, At. Data Nucl. Data Tables **64**, 253 (1996).
[7] I. Sanchez and F. Martin, J. Chem. Phys. **110**, 6702 (1999).
[8] R.C. Forrey, R. Côté, A. Dalgarno, S. Jonsell, A. Saenz, and P. Froelich, Phys. Rev. Lett. **85**, 4245 (2000).
[9] B.R. Junker, Adv. At. Mol. Phys. **18**, 207 (1982).
[10] P. Froelich, K. Szalewicz, B. Jeziorski, W. Kołos, and H.J. Monkhorst, J. Phys. B **20**, 6173 (1987).
[11] W. Kołos and L. Wolniewicz, J. Chem. Phys. **45**, 509 (1966).
[12] W. Kołos, K. Szalewicz, and H.J. Monkhorst, J. Chem. Phys. **84**, 3278 (1986).
[13] P. Froelich, B. Jeziorski, W. Kołos, H. Monkhorst, A. Saenz, and K. Szalewicz, Phys. Rev. Lett. **71**, 2871 (1993).
[14] M. Marinescu and A. Dalgarno, Z. Phys. D: At., Mol. Clusters **36**, 239 (1996).